having an output power of 5–10 W, while still having the desirable characteristics of low noise and low distortion.

V. Conclusions

The feasibility of using state-of-the-art power GaAs FET devices in the design of power amplifiers in the 6–12-GHz frequency band has been demonstrated. A unique circuit topology incorporating an edge-coupled transmission line section for input/output dc blocking has been described. This circuit topology has been shown to be capable of wide-band impedance matching for FET structures with different gate widths and different frequency ranges of operation. The measured S parameters together with this circuit topology have been used in conjunction with a computer-aided design technique to fabricate three single-stage amplifiers covering the frequency ranges of 6–10, 8–12, and 6–12 GHz. It was also shown that 1 W of CW output power can be obtained with 22-dB gain with a single-ended amplifier design. Microwave performance characteristics such as intermodulation distortion, AM-to-PM conversion, and noise figure were also presented.

Acknowledgment

The authors wish to thank D. W. Shaw and D. N. McQuiddy for many helpful discussions. They also wish to thank S. F. Goodman, L. P. Graff, and J. J. Speak for technical assistance.

References

[1] H. C. Huang, I. Drukier, R. L. Camisa, S. T. Jolly, J. Goel, and S. Y. Narayan, "GaAs MESFET performance," *Technical Digest*, pp. 235–237, 1975 International Electron Device Meeting.
[2] H. M. Macksey, R. L. Adams, D. N. McQuiddy, and W. R. Wisseman, "*X*-band performance of GaAs power FETs," *Electron. Lett.*, vol. 12, pp. 54–56, Jan. 22, 1976.
[3] R. L. Camisa, J. Goel, and I. Drukier, "GaAs MESFET linear power amplifier stage giving 1 W," *Electron. Lett.*, vol. 11, pp. 572–573, Nov. 27, 1975.
[4] F. N. Sechi and R. W. Paglione, "High-gain 1 W FET amplifier operating in *G*-band," *Digest of Technical Papers*, pp. 162–163, 1976 IEEE International Solid-State Circuits Conference.
[5] C. A. Liechti and R. L. Tillman, "Design and performance of microwave amplifiers with GaAs Schottky-gate field-effect transistors," *IEEE Trans. Microwave Theory Tech.*, vol. MTT-22, pp. 510–517, May 1974.
[6] W. H. Ku, M. E. Mokari-Bolhassan, W. C. Peterson, A. F. Podell, and B. R. Kendall, "Microwave octave-band GaAs FET amplifiers," in *IEEE Int. Microwave Symp. Dig. Tech. Papers*, 1975, pp. 69–72.
[7] H. T. Yuan, J. B. Kruger, and Y. S. Wu, "*X*-band silicon power transistor," in *IEEE Int. Microwave Symp. Dig. Tech. Papers*, 1975, pp. 73–75.
[8] H. Q. Tserng, D. N. McQuiddy, and W. R. Wisseman, "*X*-band MIC GaAs IMPATT amplifier module," *J. Solid-State Circuits*, vol. SC-10, pp. 32–39, Feb. 1975.
[9] H. Q. Tserng and D. N. McQuiddy, "*Ku*-band MIC GaAs IMPATT amplifier modules," *IEEE Int. Solid-State Circuits Conf. Digest Tech. Papers*, pp. 78–79, Feb. 1976.
[10] D. J. Mellor and J. G. Linvill, "Synthesis of interstage networks of prescribed gain versus frequency slopes," *IEEE Trans. Microwave Theory Tech.*, vol. MTT-23, pp. 1013–1020, Dec. 1975.

Design, Fabrication, and Evaluation of BARITT Devices for Doppler System Applications

JACK R. EAST, MEMBER, IEEE, HIEN NGUYEN-BA, STUDENT MEMBER, IEEE, AND GEORGE I. HADDAD, FELLOW, IEEE

Abstract—**The properties of BARITT devices and their application in self-mixing Doppler systems are presented. A detailed comparison with IMPATT and Gunn devices indicates that the BARITT is superior in this particular application in many respects, particularly when prime power requirements are important. It is shown that, even though the BARITT device will not compete with existing devices with regard to power output and efficiency, it is the best available device for self-mixed Doppler radar applications and therefore should find wide usage in such applications. Simplified design criteria for BARITT devices are given and fabrication procedures for *X*-band devices with different operating voltages are described.**

Manuscript received May 7, 1976; revised July 19, 1976. This work was supported by the Air Force Office of Scientific Research, Air Force Systems Command, U.S.A.F., under Grant AFOSR-76-2939. The United States Government is authorized to reproduce and distribute reprints for governmental purposes notwithstanding any copyright notation hereon.

The authors are with the Electron Physics Laboratory, Department of Electrical and Computer Engineering, University of Michigan, Ann Arbor, MI 48109.

I. Introduction

THE principle of operation of the *bar*rier *i*njection *t*ransit *t*ime (BARITT) device was first proposed by Shockley [1] in 1954. Recently, the first operational BARITT device was reported [2]. Since then, both theoretical and experimental data regarding small-signal as well as large-signal characteristics of the device have been reported by various authors [3]–[7]. In spite of the fact that the BARITT device is inherently a low-power and low-efficiency device, it is found to be a superior device in self-mixed doppler radar applications as compared to IMPATT and Gunn devices, and therefore should be a very useful device in these applications.

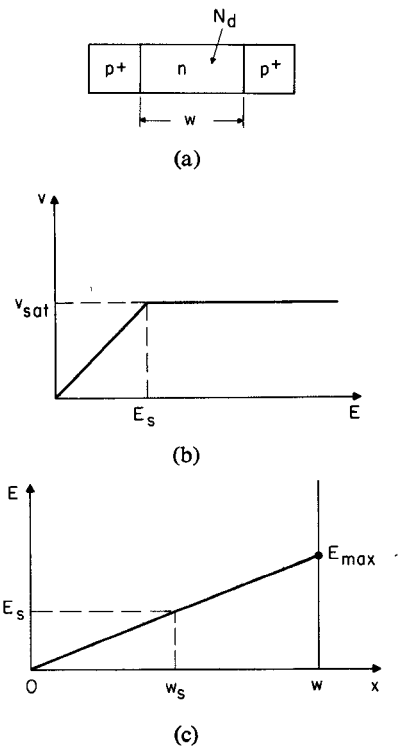

Fig. 1. Device structure, velocity electric-field characteristic, and electric field versus distance in a BARITT device.

Simplified design criteria are presented for BARITT devices based on theoretical and experimental data. Using these design criteria, different X-band BARITT devices were fabricated with operating voltages ranging from 10 to 50 V. The fabrication process is described in Section II along with the experimental results.

In Section III the self-mixing experiments are described using different BARITT devices as well as IMPATT and Gunn devices for comparison purposes. Two sets of self-mixing experiments were performed. One investigates the characteristics of the device in Doppler-radar-type applications where the modulation frequency is low and varies from 10 Hz to 50 kHz. The other set of experiments involves the receiver-type application where the IF is fixed at 30 MHz. The results are presented in detail. Comparison of the results of different BARITT devices as well as those of IMPATT and Gunn devices are described in Section IV.

II. Simplified Device Design and Fabrication Information

The BARITT devices used in this study were designed using a simplified design procedure developed by Haddad [8]. The device structure and other pertinent parameters are shown in Fig. 1 where N_d is the doping concentration in the n-layer, w is the width of the n-layer, v_{sat} is the saturated carrier velocity, E_{sat} is the field at which the velocity saturates, E_{max} is the maximum field in the device, and w_{sat} is the point where $E(x)$ equals E_{sat}. When the device is biased with a dc voltage one junction will be reverse biased and the other junction will be forward biased. At punch through most of the bias voltage appears across the reverse-biased junction. When Poisson's equation is used it can be easily shown that the voltage at which the electric field punches through is given approximately by

$$V_{PT} = \frac{1}{2}\frac{eN_d}{\varepsilon} w^2 \tag{1}$$

where

e electric charge;
ε dielectric constant.

From the theory of BARITT operation it is well known that the pulse of injected current is at the maximum voltage point. Thus the optimum transit angle is approximately $3\pi/2$. Therefore,

$$\omega\tau = \frac{3\pi}{2}$$

or

$$f\tau = \frac{3}{4} \tag{2}$$

where

f operating frequency;
τ transit time through the diode.

The transit time depends on the doping profile of the device. By assuming a uniform n-layer doping and abrupt junction for the structure in Fig. 1, a simplified expression can be derived for the transit time. It is shown in Fig. 1(b) and (c) that the carrier velocity is at v_{sat} for $E \geq E_{sat}$ and $\mu_0 E$ for $E \leq E_{sat}$, where μ_0 is the low-field carrier mobility. For $w_s \leq x \leq w$,

$$v = v_{sat}$$

and the transit time in this region is

$$\tau_1 = \frac{w - w_{sat}}{v_{sat}} \tag{3}$$

where τ_1 is the transit time from $x = w_s$ to $x = w$. When Poisson's equation is used it is found that

$$w_{sat} = \frac{E_{sat}\varepsilon}{eN_d}.$$

Equation (3) can then be expressed as

$$\tau_1 = \frac{w - (E_{sat}\varepsilon/eN_d)}{v_s}. \tag{4}$$

For $x \leq w_{sat}$,

$$v = \frac{dx}{dt}$$

$$dt = \frac{dx}{v} = \frac{dx}{\mu_0 E}$$

and

$$E = \frac{eN_d}{\varepsilon} x.$$

Therefore, the transit time from $x = 0$ to $x = w_{sat}$ is

$$\tau_2 = \int dt = \frac{\varepsilon}{eN_d\mu_0}\int_{kw_{sat}}^{w_{sat}} \frac{dx}{x} = \frac{\varepsilon}{eN_d\mu_0} \ln\frac{1}{k}. \tag{5}$$

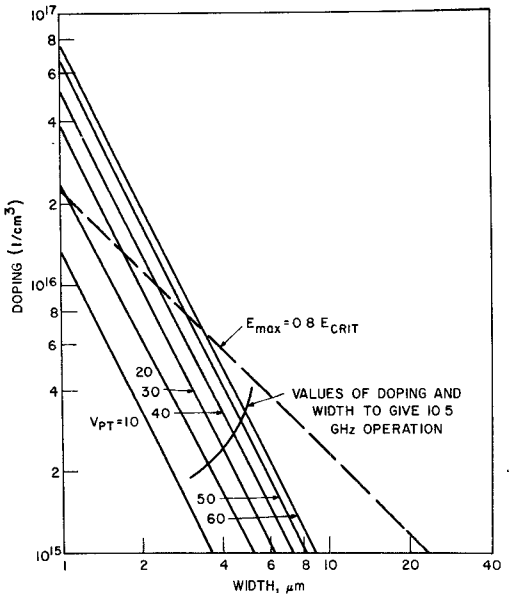

Fig. 2. Doping density versus depletion layer width for p^+-n-p^+ BARITT devices for 10.5-GHz operation.

TABLE I
SUMMARY OF BARITT DIODE INFORMATION

Voltage (V)	Doping (1/cm³)	Width (μm)	Power (mW)
50	2.5×10^{15}	5.5	25
23	1.6×10^{15}	4.5	5.4
15	1.6×10^{15}	3.6	0.52
10	1.6×10^{15}	3.0	0.15

It is noted that there is a divergent solution if the lower limit of the integration is zero. However, in an actual device the velocity at $x = 0$ is finite and not zero as implied by a zero lower limit. The parameter k is introduced to account for this finite injection velocity. Combining (2), (4), and (5) yields

$$\frac{3}{4f} = \frac{\varepsilon}{e\mu_0 N_d} \ln \frac{1}{k} + \frac{w - (E_{sat}\varepsilon/eN_d)}{v_s}. \tag{6}$$

The parameter k can be found by comparison with more exact computer results. Alternatively, the frequency predicted by (6) can be compared with experimental results to deduce k. When the experimental results of Snapp and Weissglas [3] are used, k is found to be approximately 0.02.

In a BARITT device it is desirable to have little or no ionization in the high-field region. The field in the drift region is therefore limited to

$$E_{max} \leq 0.8E_c \tag{7}$$

where E_c is the critical breakdown field.

When (1), (6), and (7) are used, various combinations of doping and width can be determined that will give optimum results at a given frequency for different bias voltages. Such results are shown in Fig. 2. A wide range of operating voltages is possible depending on the choice of the n-region doping and width. Fig. 2 and Table I were used as a guide to fabricate BARITT diodes operating between 10 and 11 GHz with operating voltages between 11 and 50 V.

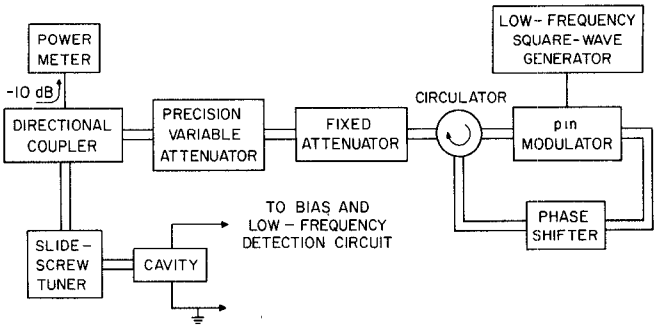

Fig. 3. RF circuit diagram.

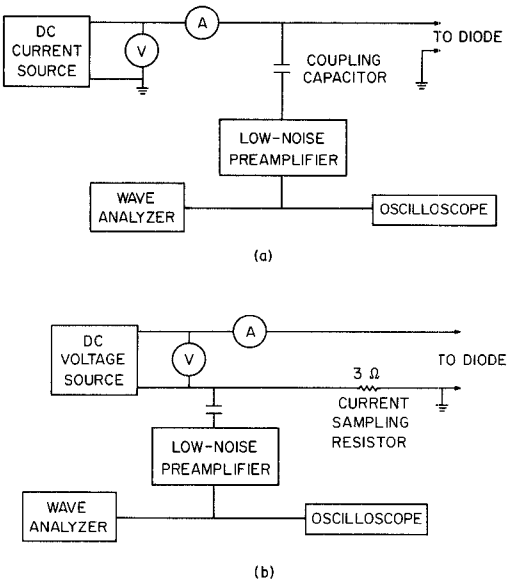

Fig. 4. Bias and detection circuits for (a) BARITT and IMPATT devices and (b) the Gunn device.

The diodes were fabricated from n-p^+ Si epitaxial wafers with boron nitride sources used for the p^+ diffusions. Standard photoetching techniques were used to form the diodes which were mounted and tested in S-4-type packages.

III. Results of Self-Mixing Experiments

A. Doppler Radar Experiments

1. Experimental Setup: Fig. 3 shows a block diagram of the RF circuit. The low-frequency detection circuit for the BARITT and IMPATT devices is shown in Fig. 4(a), and for the Gunn device, in Fig. 4(b). The difference in detection schemes is due to the fact that voltage is measured in the case of the BARITT and IMPATT whereas a current is measured for the Gunn device.

In the RF circuit the oscillator power is attenuated and fed through a pin modulator by means of a circulator. The signal is 100 percent square-wave modulated and returns to the oscillator after being further attenuated. At the oscillator the returned signal is mixed with the oscillator signal itself and the downconverted signal is picked up in the bias circuit. The total round-trip attenuation is calibrated so

that the return signal power level can be computed from the oscillator output power. In the bias circuit, the low-frequency signal is picked up by a coupling capacitor and amplified. The output of the amplifier is connected to an oscilloscope for observation and to a wave analyzer with variable center frequency and bandwidth, where the true rms value of the noise and signal can be measured.

2. Method of Measurement: The BARITT and IMPATT devices are biased by a current source and the signal is detected by measuring the low-frequency voltage across the device. For the Gunn diode, a voltage source is used for biasing and the signal is detected by a current sampling resistor. The principal parameter in determining the sensitivity of a self-mixing oscillator is the minimum detectable signal (MDS) power level, that is, how weak a signal the device can detect. This MDS is affected not only by the noise of the system but also by the mixing characteristics of the device as well as the bandwidth of the system. The noise figure of the system is related to its MDS by the following relation:

$$\text{MDS} = kTB \cdot \text{NF}$$

where

MDS	minimum detectable signal power;
k	Boltzmann's constant;
T	temperature in degrees Kelvin;
B	bandwidth in hertz;
NF	noise figure.

The following procedure was applied to all devices in measuring the MDS. The oscillating diode is tuned by both the bias and the RF circuits to achieve the desired operating point. Care is taken so that no spurious oscillations or bias circuit instabilities are present. The wave analyzer center frequency is tuned to the modulation frequency applied at the pin modulator. Bandwidths of 10, 100, and 1000 Hz were used for modulation frequencies ranging from 30 to 50 Hz, 1 to 5 kHz, and 10 to 50 kHz, respectively. The RF circuit attenuation is then set at maximum so that no signal is returned and the detected rms voltage is pure noise. The attenuation is then decreased until the detected signal level is 3 dB above that of the noise alone. At this point the signal power is equal to the noise power and the return RF power is defined as the MDS power level measured in decibels referred to 1 mW.

3. Results: For uniformity the MDS is given for a normalized bandwidth of 1 Hz. Different BARITT devices with voltages ranging from 10 to 50 V were tested. All of these BARITT diodes were fabricated here. For each device the MDS is measured as a function of the modulation frequency. The performance of the 50-V BARITT device at different output-power levels varying from low (0.1 mW) to near maximum (10 mW) is shown in Fig. 5. Fig. 6 shows the MDS of the same device as a function of bias current while the RF circuit remains fixed and the modulation frequency is kept at 1 kHz. This illustrates that bias variation is not very critical to BARITT performance, which is not the case with either the IMPATT or Gunn devices tested in this experiment. The performance of the 23-, 15-, and 10-V BARITT devices is plotted in Figs. 7, 8, and 9, respectively.

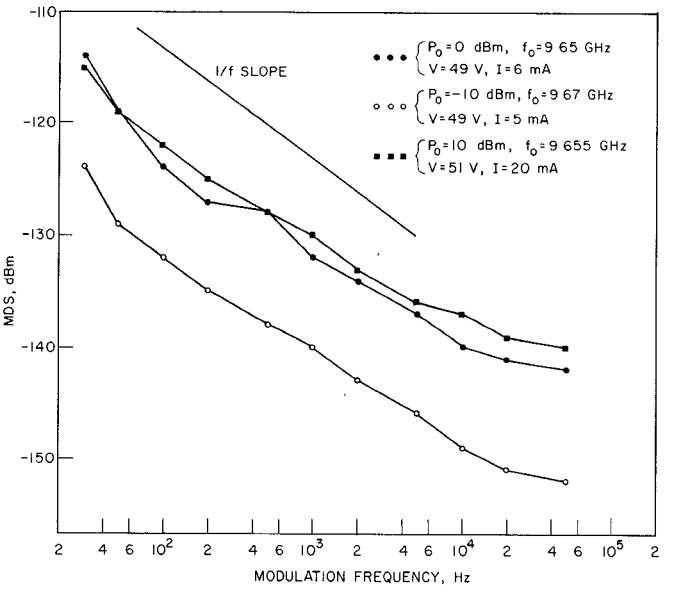

Fig. 5. MDS in a 1-Hz bandwidth versus Doppler frequency for a 50-V BARITT oscillator.

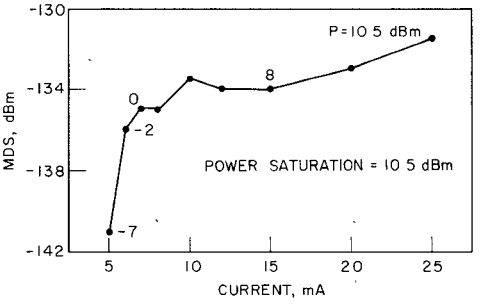

Fig. 6. MDS as a function of bias current for a BARITT device, RF circuit fixed (modulation frequency = 1 kHz and bandwidth = 1 Hz).

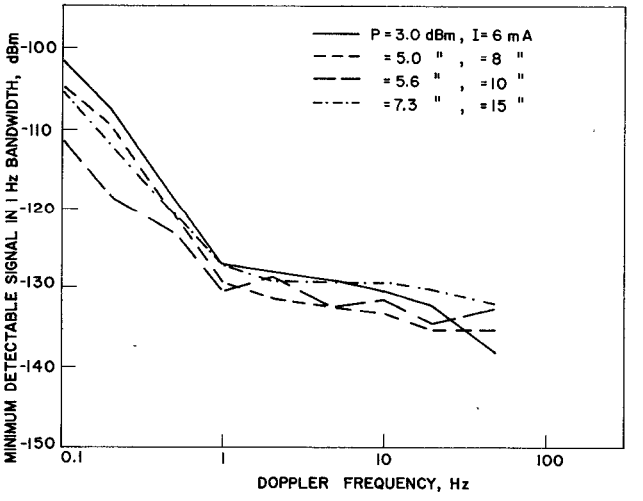

Fig. 7. MDS in a 1-Hz bandwidth versus Doppler frequency for a 23-V BARITT oscillator (f_0 = 10.1 GHz).

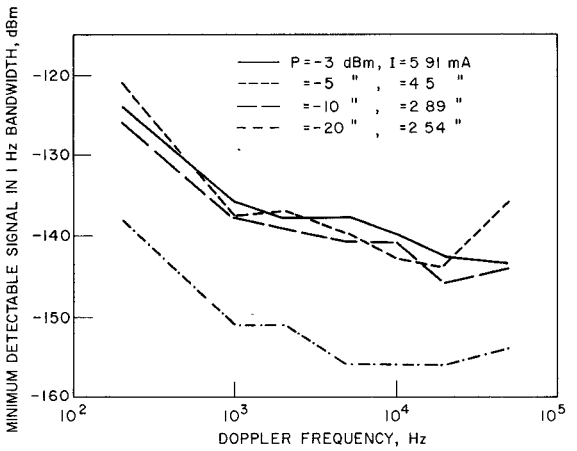

Fig. 8. MDS versus Doppler frequency for a 15-V BARITT ($f_0 \simeq$ 9 GHz).

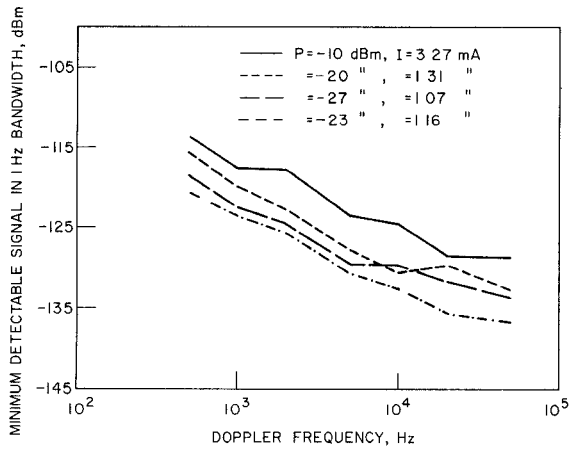

Fig. 9. MDS in a 1-Hz bandwidth versus Doppler frequency for a 10-V BARITT oscillator (f_0 = 11 GHz).

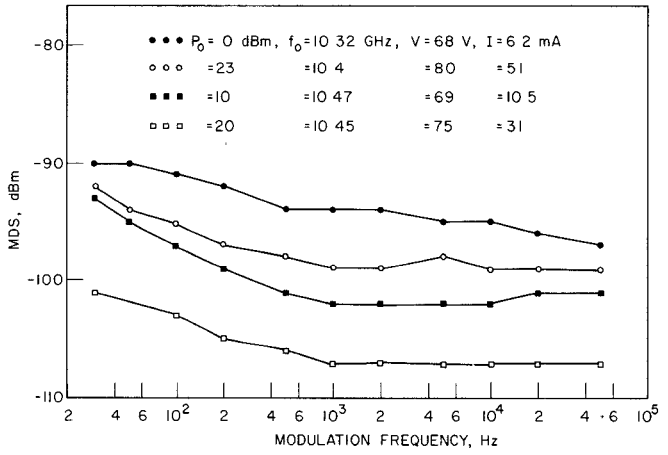

Fig. 10. MDS versus modulation frequency for an IMPATT device (bandwidth = 1 Hz).

A commercial IMPATT diode was used in the test, and its performance is shown in Fig. 10. The MDS versus modulation frequency is plotted for output-power levels varying from 1 to 200 mW. For the Gunn device, which is also a typical commercial diode, the MDS versus modulation frequency is shown in Fig. 11 with an output power varying from 10 to above 30 mW.

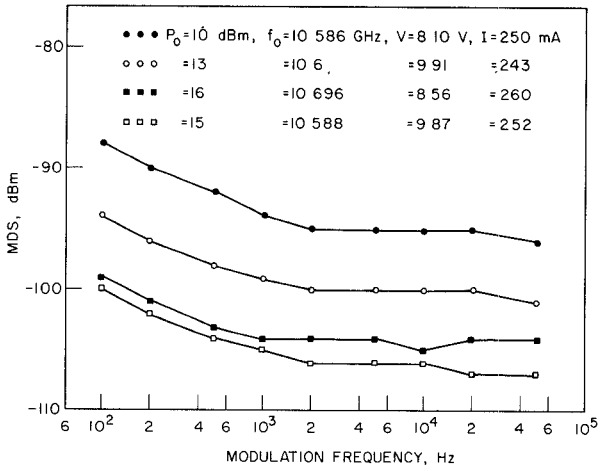

Fig. 11. MDS versus modulation frequency for a Gunn device (bandwidth = 1 Hz).

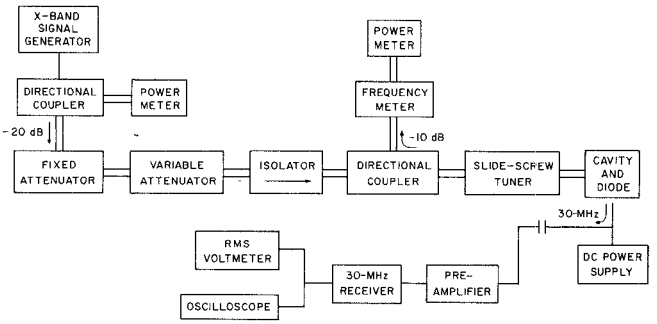

Fig. 12. Block diagram of 30-MHz receiver experiment.

B. Receiver Experiment

In this experiment the incoming signal is generated by an external source which is set 30 MHz away from the self-mixing oscillator frequency. As in the previous experiment, the MDS is measured with a bandwidth of 10 MHz.

1. Experimental Setup: Fig. 12 shows a block diagram of the experimental setup. In this case an *X*-band generator is used as the external signal source. The signal is square-wave modulated at 1 kHz to facilitate measurements and is attenuated before it reaches the self-mixing oscillator. An isolator keeps this oscillator isolated from the signal source. The intermediate frequency is picked up in the bias circuit, in the same fashion as the previous experiment, amplified, and detected by a video detector built in to the amplifier. This video output is then measured by a true rms voltmeter.

2. Procedure: As in the previous experiment, the attenuation is first set at maximum to measure the noise level. It is then decreased until the detected signal is 3 dB above the noise level, and the incoming signal power level is determined by the external generator output power and the total attenuation.

3. Results: Fig. 13 shows the MDS of the three devices, BARITT, IMPATT, and Gunn, as a function of the output power. Besides being superior to both the IMPATT and the Gunn devices at any power level, the BARITT devices also show that the MDS becomes lower at lower output power while the converse is true for both the Gunn and IMPATT devices.

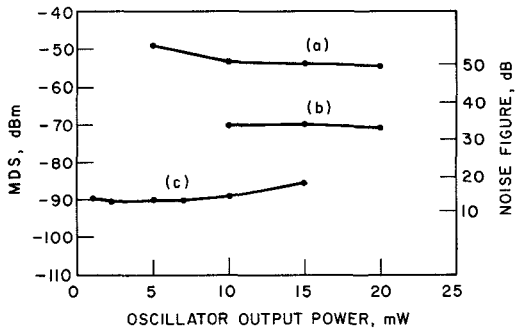

Fig. 13. MDS at different output-power levels. (a) IMPATT device. (b) Gunn device. (c) BARITT device (bandwidth = 10 MHz, IF = 30 MHz).

IV. Discussion of Results

In terms of sensitivity, the BARITT device is superior at any power level and modulation frequency. An outstanding characteristic of the device is that the sensitivity is better at lower oscillator output-power levels while the reverse is true for both the Gunn and IMPATT devices. In addition, the sensitivity of the low-voltage BARITT device is comparable or better than that of the higher voltage ones. This is an important feature and a definite advantage over the other devices. Another desirable quality of the BARITT device is its insensitivity to bias variation, as can be seen in Fig. 6. This is not true for the Gunn or IMPATT devices where a slight variation in bias leads to a rapid deterioration of sensitivity. To offset this the RF circuit has to be retuned whenever the bias is slightly changed.

It is also apparent that the BARITT device does seem to possess a $1/f$ noise component. The origin of this $1/f$ noise in BARITT devices is not well understood at this time. One hesitates to conclude that it is an inherent characteristic. If this $1/f$ noise were due to some effect of the fabrication process, then eventually it could be eliminated or reduced by more sophisticated techniques of fabrication. This would greatly enhance the sensitivity of the BARITT device at the low-modulation frequency range.

V. Conclusion

It has been shown that, using the simplified design principle given here, BARITT devices of different operating voltages and frequencies can be successfully designed. While a great deal more remains to be learned about the noise and mixing characteristics of the BARITT device, the experiments described show that the BARITT device has definite advantages in self-mixing mode applications. These are, in short, low-power consumption, high sensitivity, and ease of fabrication and operation. The BARITT device also has great potential in the higher frequency region due to the fact that low output power does not affect its sensitivity.

References

[1] W. Shockley, "Negative resistance arising from transit time in semiconductor diodes," *Bell System Tech. J.*, vol. 33, pp. 799–826, July 1954.
[2] D. J. Coleman, Jr., and S. M. Sze, "A low-noise metal–semiconductor–metal (MSM) microwave oscillator," *Bell System Tech. J.*, vol. 50, pp. 1695–1699, May/June 1971.
[3] C. P. Snapp and P. Weissglas, "On the microwave activity of punchthrough injection transit-time structure," *IEEE Trans. Electron Devices*, vol. ED-19, pp. 1109–1118, Oct. 1972.
[4] S. P. Kwok, H. Nguyen-Ba, and G. I. Haddad, "Properties and potential of BARITT devices," *IEEE Int. Solid-State Circuits Conf. Digest*, Philadelphia, PA, pp. 180–181, Feb. 1974.
[5] D. J. Coleman, Jr., "Transit-time oscillations in BARITT diodes," *J. Appl. Phys.*, vol. 43, pp. 1812–1819, April 1972.
[6] A. Sjölund, "Small-signal noise analysis of punch-through injection microwave diodes," *Solid-State Electronics*, vol. 16, pp. 559–569, May 1973.
[7] G. T. Wright, "Small-signal characteristics of semiconductor punch-through injection and transit time diodes," *Solid-State Electronics*, vol. 16, pp. 903–912, August 1973.
[8] G. I. Haddad, "Basic principles and simple design procedures of BARITT devices," EPL Memo No. 75-2-005030, Electron Physics Laboratory, The University of Michigan, Ann Arbor, June 1975.

Millimeter-Wave Receivers with Subharmonic Pump

THOMAS F. McMASTER, MARTIN V. SCHNEIDER, FELLOW, IEEE, AND WILLIAM W. SNELL, JR.

Abstract—**Hybrid integrated downconverters which are pumped at half the frequency needed in a conventional downconverter have shown a conversion loss of 3 dB at 50 GHz and 6 dB at 100 GHz with a corresponding single-sideband (SSB) receiver noise figure of 7 dB at 50 GHz and 11 dB at 100 GHz. The circuits are linearly scaled from an optimized 5-GHz model. Each downconverter consists of a stripline conductor pattern, a novel transition from waveguide to stripline, and a Schottky-barrier diode pair. The circuits can be tuned over a useful RF bandwidth of 20 GHz, and they can be readily scaled to other frequency bands.**

Manuscript received May 13, 1976; revised July 23, 1976.
The authors are with Bell Laboratories, Holmdel, NJ 07733.

I. Introduction

A NEW subharmonically pumped downconverter has shown a conversion loss and an RF bandwidth which is superior to the performance of previously reported integrated converters [1], [2] and of conventional wave-